

Association of Visual Function Measures with Drusen Volume in Early Stages of Age-Related Macular Degeneration

Susanne G. Ponderfer,¹ Maximilian W. M. Wintergerst,¹ Shekoufeh Gorgi Zadeh,^{2,3} Thomas Schultz,^{2,4} Manuel Heinemann,¹ Frank G. Holz,¹ and Robert P. Finger¹

¹Department of Ophthalmology, University of Bonn, Bonn, Germany

²Department of Computer Science, University of Bonn, Bonn, Germany

³Department of Medical Biometry, Informatics and Epidemiology, University of Bonn, Bonn, Germany

⁴Bonn-Aachen International Center for Information Technology, University of Bonn, Bonn, Germany

Correspondence: Robert P. Finger, Department of Ophthalmology, University of Bonn, Ernst-Abbe-Str. 2, D-53127 Bonn, Germany; robert.finger@ukbonn.de.

Received: October 28, 2019

Accepted: February 1, 2020

Published: March 30, 2020

Citation: Ponderfer SG, Wintergerst MWM, Gorgi Zadeh S, et al. Association of visual function measures with drusen volume in early stages of age-related macular degeneration. *Invest Ophthalmol Vis Sci.* 2020;61(3):55. <https://doi.org/10.1167/iovs.61.3.55>

PURPOSE. To assess which visual function measures are most strongly associated with overall retinal drusen volume in age-related macular degeneration (AMD).

METHODS. A total of 100 eyes (16 eyes with early AMD, 62 eyes with intermediate AMD, and 22 eyes from healthy controls) were recruited in this cross-sectional study. All subjects underwent several functional assessments: best-corrected visual acuity (BCVA), low-luminance visual acuity (LLVA), visual acuity (VA) measured with the Moorfields Acuity Chart (MAC-VA), contrast sensitivity with the Pelli-Robson test, reading speed using the International Reading Speed texts, and mesopic and dark-adapted microperimetry. Drusen volume was automatically determined based on optical coherence tomography using an approach based on convolutional neural networks. The relationship between drusen volume and visual function was assessed with linear regressions controlling for confounders.

RESULTS. Mean drusen volume and MAC-VA differed significantly among all AMD stages and controls ($P < 0.001$). In univariate linear regression, LLVA, MAC-VA, contrast sensitivity, and mesopic and dark-adapted microperimetry were significantly negatively associated with the overall drusen volume (all $P < 0.006$). After controlling for AMD stage, age, and the presence of subretinal drusenoid deposits, MAC-VA and mesopic and dark-adapted microperimetry were still significantly associated with drusen volume ($P = 0.008$, $P = 0.023$, and $P = 0.022$, respectively).

CONCLUSIONS. Our results suggest that MAC-VA, as well as mesopic and dark-adapted microperimetry, might indicate structural changes related to drusen volume in early stages of AMD.

Keywords: Automatic segmentation of drusen, drusen volume, age-related macular degeneration, contrast sensitivity

Age-related macular degeneration (AMD) is the leading cause of visual impairment in the elderly in developed countries, with a worldwide prevalence of 8.1% for early AMD and 8.69% for any AMD in people over 45 years of age.^{1,2} Due to current demographic trends, the burden of AMD is estimated to grow to 288 million by 2040.¹ Late stages can lead to a severe loss of visual acuity, whereas early stages of the disease are often not associated with obvious visual symptoms. In conventional visual function tests under high luminance and high contrast, patients with early and intermediate stages of the disease usually achieve good scores; however, they often report difficulties and vision loss under low lighting, low contrast, and changing light conditions.³⁻⁵ Therefore, standardized visual function tests under low luminance and low contrast have attracted increasing interest, particularly with regard to early stages of AMD, as

they might allow better monitoring of the disease and aid in predicting disease progression.⁶

Usually the first clinical sign of AMD are drusen located between the basal lamina of the retinal pigment epithelium (RPE) and the inner collagenous layer of Bruch's membrane (BM), in the sub-RPE-basal laminar space.^{7,8} Retinal cells overlying drusen exhibit structural and molecular abnormalities indicative of photoreceptor degeneration and Müller glial activation, suggesting that photoreceptor cell function is compromised as a consequence of drusen formation.⁹ Drusen are among the most important biomarkers for staging AMD.¹⁰⁻¹³ A recently developed convolutional neural network (CNN)-based approach for a fully automated segmentation of drusen in optical coherence tomography (OCT) images¹⁴ allows us to compute the overall drusen volume. Compared to manual segmentation of drusen,



automated segmentation has been shown to be highly reproducible and accurate.^{15,16} The relationship between visual function tests under low luminance and low contrast and measurements of retinal structure associated with AMD progression, such as drusen volume, has not been well described so far. It may be that structural and functional measures provide complementary information about disease status. Thus, we evaluated the relationship between drusen volume and a battery of visual function tests under low luminance and low contrast.

METHODS

We conducted a cross-sectional study at the Department of Ophthalmology, University of Bonn, Germany, from January 2017 until January 2019. The study was approved by the Institutional Review Board of the University Bonn (approval ID 013/16). Written informed consent was obtained from all participants following an explanation of all non-invasive tests involved. The protocol followed the tenets of the Declaration of Helsinki.

Sixteen eyes from patients with early AMD, 62 eyes from patients with intermediate AMD (iAMD), and 22 healthy eyes were recruited from patients from the AMD outpatient clinic, the self-help organization Pro Retina, and family members of patients. Participants were categorized as early AMD, iAMD, or healthy controls (no apparent aging changes and normal aging changing), based on the classification system introduced by Ferris et al.¹¹ Exclusion criteria were age < 50 years; any media opacity that could compromise vision; amblyopia, diabetes, glaucoma, or neurological or systemic disease affecting vision; refractive errors > 6.00 diopters (D) of spherical equivalent; and >2.00 D of astigmatism. Spectral-domain OCT (SD-OCT) raster scanning was performed using a 20° × 25° scan field (121 B-scans, automated real-time mode 20 frames, centered on the fovea); fundus autofluorescence (FAF) and infrared reflectance (IR) imaging (Spectralis OCT2, Heidelberg Engineering, Heidelberg, Germany); and color fundus photography (CFP) of the macula (Canon CR-2 AF; Tokyo, Japan). For a diagnosis of subretinal drusenoid deposits (SDDs) and pigment changes, characteristic changes had to be present on at least two imaging methods including CFP, SD-OCT, FAF, and IR. All patients also underwent a clinical examination including dilated funduscopy. Pupillary dilatation was achieved using 1% tropicamide.

Functional Testing

All participants underwent the following visual function tests: best-corrected visual acuity (BCVA), Early Treatment Diabetic Retinopathy Study (ETDRS) letters, low-luminance visual acuity (LLVA), Moorfields Acuity Chart (MAC-VA), contrast sensitivity measurement using Pelli–Robson charts, reading speed using the International Reading Speed Texts (IREST), and mesopic and dark-adapted microperimetry using modified Macular Integrity Assessment (S-MAIA) microperimetry (CenterVue, Padova, Italy).

BCVA for letters was assessed according to the ETDRS method¹⁷ at a testing distance of 4 meters. LLVA was assessed in the same manner, but with a 2.0-log unit neutral density filter that reduces luminance by 100-fold¹⁸ placed in the trial frame. MAC-VA measurement followed the same procedure as for BCVA. The MAC charts are based on the ETDRS

charts and employ a high-contrast, high-pass letter design with a gray background of the same mean luminance as the letters to simulate lower contrast situations.¹⁹ The letters are also referred to as vanishing optotypes, because, for normal vision, the detection and recognition thresholds are very similar, and the letters seem to disappear soon after the recognition limit has been reached.¹⁹ Contrast sensitivity was measured using a Pelli–Robson chart presented at a distance of 1 meter.^{20–22} For the IREST, patients wore their best near correction and were asked to read one paragraph aloud while they were timed with a stopwatch.²³ BCVA and reading speed were performed under photopic conditions, whereas LLVA, MAC-VA, and contrast sensitivity were performed under mesopic conditions. Based on the test characteristics and the lighting conditions in which these tests were administered, we presumed a more cone-mediated function in the BCVA and reading test and a partially rod-mediated function in the LLVA, MAC-VA, contrast sensitivity, and, in particular, mesopic microperimetry.

Prior to microperimetry testing with the S-MAIA device, pupillary dilatation was performed. The S-MAIA performs fundus tracking using a line-scanning laser ophthalmoscope with a super-luminescent diode illumination with a central wave light of 850 nm for mesopic testing and an additional light-emitting diode projecting red (627 nm) stimuli for dark-adapted testing. The dark-adapted testing with red (627 nm) stimuli is more influenced by cone-mediated function, reflecting a mixture of both rod- and cone-mediated responses.²⁴ As previously described, a customized stimulus grid was used that consisted of 33 points located at 0°, 1°, 3°, 5°, and 7° from fixation.²⁵ First, mesopic testing was performed. Patients were not dark-adapted, but the room light was switched off just before the examination. After mesopic testing, patients underwent 30 minutes of dark adaptation while waiting in the examination room (light was switched off, light level was <0.1 lux), and then dark-adapted testing was performed. The microperimetric outcome measure was the global mean sensitivity (in dB) and mean sensitivity at eccentricities of 0°–1°, 3°, 5°, and 7°. All tests were performed in one eye, with the non-study eye covered with an eye patch.

Automatic Segmentation of Drusen

For automated segmentation of drusen, the pipeline reported by Gorgi Zadeh et al.¹⁴ was used. In the first step, this drusen segmentation pipeline automatically segments RPE and BM bands, using a CNN, which transforms an input B-scan into RPE and BM probability maps. For the final hard segmentation of RPE and BM bands, probability maps are converted into cost maps so that pixels with higher probability have lower costs. Dijkstra's algorithm is used to find a path with the minimum accumulated costs from the left to the right of each map.²⁶ The extracted paths are considered as final RPE and BM band segmentation.

In the second step, an ideal (normal) RPE is estimated through a rectification of RPE and BM bands.¹⁴ In the rectification step, both RPE and BM are shifted vertically and column-wise until the BM band becomes a straight horizontal line, then a low-degree polynomial is fitted on the shifted RPE band and transformed back into the original image coordinates and is regarded as the drusen-free RPE. Finally, any area between the RPE and drusen-free RPE is classified as drusen. To eliminate falsely detected drusen, those with a height of 2 pixels or less are removed from the final

TABLE 1. Characteristics of Participants in Each Group

Characteristic	AMD Group		
	Control	Early	Intermediate
Age (y), mean \pm SD	59.8 \pm 6.3	70.0 \pm 6.7	69.7 \pm 7.3
Eyes, n	22	16	62
Women, n (%)	13 (59.1)	11 (68.80)	42 (67.7)
Subretinal drusenoid deposits, n (%)	0	5 (31.3 %)	12 (19.4)
Pigment changes, n (%)	0	0	31 (50)

segmentation. More details on the automated drusen segmentation pipeline can be found in the Supplementary Material.

Statistical Analysis

Descriptive statistics were performed to assess baseline demographic variables for the AMD groups and controls. Due to the sample size, most results were not normally distributed (by the Shapiro–Wilk test), so non-parametric tests were used for analysis. The Kruskal–Wallis test was used for group comparisons. Pairwise differences were calculated using the nonparametric Wilcoxon rank-sum test. The relationship between drusen volume and demographic variables was assessed with univariate linear regression. In the overall cohort, separate univariate linear regression models against drusen volume were performed for each of the visual functional tests. If the relationship between a functional test and average person measures reached a $P < 0.05$ in univariate analysis, multiple regression was used to ensure that the findings were not confounded by different demographic characteristics across groups. Statistical analyses were performed using the statistical software SPSS Statistics (IBM, Armonk, NY, USA).²⁷ $P < 0.05$ was considered statistically significant.

RESULTS

Sociodemographic and Clinical Characteristics of the Participants

The 100 eyes studied included 16 eyes with early AMD (16%), 62 eyes with iAMD (62%), and 22 eyes from healthy controls (22%). The mean age of participants was 67.5 ± 8.1 years, and there were more female participants (66%) than male. The controls were significantly younger than the early AMD and iAMD patients ($P < 0.001$), but there was no significant difference in age between the two AMD groups ($P = 0.88$) (Table 1). Mean image quality of our sample was 30.158 dB (SD 4.395). Mean drusen volume was found to be close to zero for controls (0.00024 ± 0.0003 mm³). For early AMD, mean drusen volume was higher (0.00272 ± 0.0015 mm³), and volume was again higher for iAMD (0.13582 ± 0.1945 mm³). Age was not significantly associated with drusen volume ($P = 0.642$). Early AMD and iAMD patients were found to have a significantly larger drusen volume when compared to controls (each $P < 0.001$), and iAMD patients also had significantly larger drusen volume compared to early AMD ($P < 0.001$) (Fig.). SDDs were present in five eyes with early AMD (31.3 %) and in 12 eyes with iAMD (19.4%) but not in control eyes. Pigment changes were present in 31 eyes with iAMD (50%). All functional vision tests were significantly decreased in iAMD compared

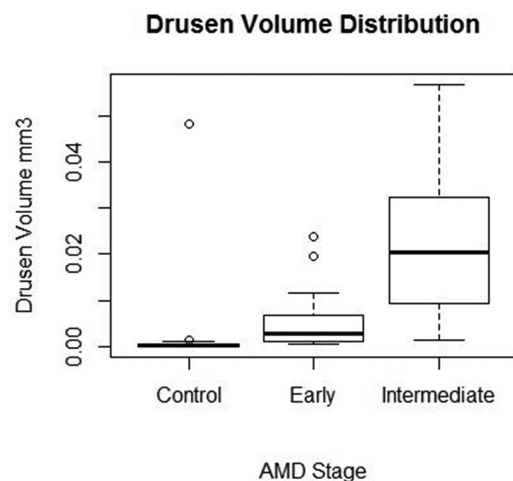


FIGURE. Boxplot showing drusen volume (in mm³) for controls and early and intermediate AMD (excluding outliers). Each boxplot includes the maximum (upper whisker), upper quartile (top of the box), median (horizontal line in box), lower quartile (bottom of the box), and minimum (lower whisker) values.

to controls (all $P < 0.05$). BCVA and MAC-VA were also significantly decreased in early AMD compared to controls ($P = 0.016$ and $P = 0.006$, respectively), but there was no significant difference in all other functional tests between the two groups (all $P > 0.05$). When comparing early AMD to iAMD, BCVA and reading speed did not differ significantly ($P = 0.31$ and $P = 0.07$, respectively), but there was a significant decrease in LLVA, MAC-VA, contrast sensitivity, and mesopic and dark-adapted microperimetry in the iAMD group compared with the early AMD group (all $P < 0.05$) (Table 2). Univariate linear regression revealed no significant association between drusen volume and age (β coefficient = 0.001; $P = 0.642$).

Relationship Between Drusen Volume and Visual Function Tests

In univariate linear regression, LLVA, MAC-VA, contrast sensitivity, and mesopic and dark-adapted microperimetry were significantly negatively associated with the overall drusen volume (all $P < 0.006$) (Table 3). After controlling for AMD stage, age, and the presence of SDD, MAC-VA and global mesopic and dark-adapted microperimetry were still significantly associated with drusen volume ($P = 0.008$, $P = 0.023$, and $P = 0.022$, respectively). For mesopic and dark-adapted microperimetry, mean sensitivity at 0°–1° and 3° degrees was significantly associated with drusen volume, whereas mean sensitivity at 5° and 7° was not associated with drusen volume after adjusting for AMD stage, age, and the presence

TABLE 2. Descriptive Analysis and Group Comparisons

	Mean (SD)			P*		
	Control	Early AMD	iAMD	Early AMD vs. iAMD	Early AMD vs. Control	iAMD vs. Control
Drusen load, mm ³	0.000236 (0.0003033)	0.002718 (0.0015339)	0.135821 (0.1945323)	<0.001	<0.001	<0.001
BCVA	87.6 (4.1)	83.5 (4.1)	81.6 (6.8)	0.306	0.016	<0.001
LLVA	74.0 (4.6)	70.0 (6.4)	64.0 (9.3)	0.008	0.06	<0.001
MAC-VA	68.4 (3.9)	64.1 (4.2)	60.1 (6.7)	0.026	0.006	<0.001
Contrast sensitivity	38.2 (2.9)	37.0 (3.6)	33.6 (3.1)	<0.001	0.137	<0.001
IReST	166.8 (21.9)	162.7 (23.9)	149.6 (28.1)	0.077	0.693	0.012
Mesopic microperimetry	26.2 (1.7)	24.9 (3.2)	23.0 (2.8)	0.016	0.056	<0.001
Dark-adapted microperimetry	22.7 (1.4)	23.1 (5.7)	20.5 (2.4)	0.004	0.715	<0.001

* P values are based on the Wilcoxon rank-sum test. Bold numbers indicate statistical significance.

TABLE 3. Linear Regression of Visual Function Measures Against Drusen Volume (in mm³)

	Univariate Regression		Adjusted for AMD Stage and Age		Adjusted for AMD Stage, Age, and Presence of SDD	
	β Coefficient	P	β Coefficient	P	β Coefficient	P
BCVA	-0.001	0.571	0.001	0.581	0.001	0.588
LLVA	-0.005	0.007	-0.003	0.091	-0.003	0.093
MAC-VA	-0.009	<0.001	-0.007	0.008	-0.007	0.008
Contrast sensitivity	-0.014	0.001	-0.007	0.148	-0.008	0.130
IReST	-0.001	0.125	0.000	0.368	-0.000	0.349
Mesopic microperimetry						
Global	-0.019	0.001	-0.012	0.040	-0.014	0.023
0°-1°	-0.022	<0.001	-0.018	<0.001	-0.018	<0.001
3°	-0.018	<0.001	-0.012	0.015	-0.015	0.006
5°	-0.012	0.033	-0.005	0.306	-0.007	0.195
7°	-0.007	0.130	-0.001	0.784	-0.001	0.609
Dark-adapted microperimetry						
Global	-0.017	0.001	-0.011	0.022	-0.012	0.022
0°-1°	-0.016	<0.001	-0.010	0.031	-0.010	0.037
3°	-0.021	<0.001	-0.016	0.001	-0.017	0.001
5°	-0.010	0.029	-0.006	0.185	-0.006	0.166
7°	-0.005	0.270	-0.001	0.983	-0.000	0.951
Pigment changes	0.089	0.013	0.038	0.319	0.034	0.372

Bold numbers indicate statistical significance.

of SDD (Table 3). In univariate regression, the presence of pigment changes was significantly associated with drusen volume (P = 0.013), but adjusting for pigment changes in multivariate regression showed no effect on overall results.

DISCUSSION

In our study, drusen volume was associated with visual impairment detected in functional tests under low luminance and challenging contrast conditions in early stages of AMD. Specifically, MAC-VA and both mesopic and dark-adapted microperimetry were significantly associated with drusen volume. These results indicate a structure-function relationship in early stages of AMD that may not be detectable using conventional high-luminance, high-contrast functional tests.

The association between drusen volume and microperimetric sensitivity found in this study is consistent with previous studies in early stages of AMD²⁸⁻³¹; however, in those studies only mesopic microperimetry was assessed. We also found global dark-adapted microperimetric sensitivity, as well as sensitivities at 0°-1° and 3° eccentric-

ities but not at 5° and 7° eccentricities, to be associated with drusen volume. Our results revealed a significant association between MAC-VA and drusen volume. We also found that MAC-VA was the only functional test that differed significantly among all three groups. When comparing the iAMD group to controls, we found that the performance of all visual function tests decreased significantly in the iAMD group. These findings are comparable with previous studies that have also reported a reduced visual function in these tests. Chandramohan and colleagues³² also found BCVA, LLVA, and mesopic microperimetry significantly decreased in patients with iAMD compared to healthy controls. Similar results were found by Wu et al.,³⁵ who found that results of these tests were significantly reduced for all AMD groups except early AMD compared to controls, which is in line with our results. BCVA was on average four letters worse in eyes with early AMD, and this difference was statistically significant. This is comparable to the findings from Owsely et al.³⁴ and Klein et al.,³⁵ who reported a significant difference of two letters between these two groups. We did not find a significant relationship between the presence

of SDDs and drusen volume, and adjusting for SDDs in multivariate regression analysis demonstrated no changes in the results. Interestingly, we found a higher prevalence of SDDs in eyes with early AMD (31.3%) than in eyes with iAMD (19.4%), which is in contrast to many other studies and likely a spurious finding due to our small sample size.³⁶

We found that LLVA and contrast sensitivity were decreased in the iAMD group compared to controls and early AMD; however, we did not find a significant difference in these functional tests between early AMD and controls. Puell et al.³⁷ showed that LLVA was impaired in early stages of AMD before changes in BCVA were observed. Decreased contrast sensitivity in early AMD compared to healthy controls has been reported by Feigl and coworkers.³⁸

In our study, drusen volume was found to be largest in the iAMD group and significantly lower in the early AMD group and controls. This is in accordance with several other studies demonstrating that drusen volume increases with increasing AMD stage and is predictive of progression to late AMD.^{39–41} For early AMD, we calculated a mean drusen volume of 0.0027 mm³, which is lower than the values reported by Lei and coworkers,⁴² who found a mean drusen volume of 0.03 (range, 0.00–0.28) in eyes with early AMD. This could also be explained by the small sample size in our early AMD group. The mean drusen volume measure we obtained for the iAMD group of 0.138 mm³ is comparable to the results of a study by Yehoshua et al.,⁴³ who reported drusen volume measures of 0.095 to 0.375 mm³ in the highest quintile for eyes with nonexudative AMD.

We showed that drusen volume is associated with visual impairment detected by functional tests. This is in line with previous studies that have found that functional tests under low lighting are correlated with retinal morphology in AMD.^{44,45}

Strengths of our study include the comprehensive panel of functional tests, including the relatively new MAC charts, for which few data are available, as well as the use of reading performance and dark-adapted microperimetry. All participants were phenotyped according to the current reference-standard retinal imaging in combination with a clinical examination. For drusen volume calculation, we used a new CNN-based approach that allows for the fully automated segmentation of drusen in OCT images. Gorgi Zadeh et al.¹⁴ demonstrated that the CNN-based approach yields much better results than a previous state-of-the-art method reported by Chen et al.⁴⁶ and therefore allows for accurate automated assessment of drusen load in AMD. A limitation of our study is the relatively small sample size of the early AMD group and the controls, leading to less statistical power. As common with exploratory studies, no adjustment for multiple testing was done which might lead to an overestimation of statistical power. Another limitation of our study is the fact that the control group was younger than both AMD groups, although univariate linear regression revealed no significant association between age and drusen volume ($P = 0.642$), and we adjusted for age in the multivariate regression analyses.

In conclusion, our study showed that MAC-VA and mesopic and dark-adapted microperimetry are associated with drusen volume in early stages of AMD and thus might provide an indication of structural changes. Our findings suggest that these visual function tests might be useful measurements in monitoring and diagnosing early AMD and iAMD and could be used as functional endpoints in clinical

studies. However, more research is warranted, and a longitudinal follow-up will be needed to evaluate the performance of these functional tests as intended, for example, by the MACUSTAR consortium.⁴⁷

Acknowledgments

We thank Jeany Q. Li, Matthias M. Mauschitz, Maximilian Pfau, Christopher A. Turski, and Gabrielle N. Turski for their support in conducting the ophthalmic examinations.

This research was supported by the German Scholars Organization/Else Kröhner Fresenius Stiftung (GSO/EKFS 16) and BONFOR GEROK Program, Faculty of Medicine, University of Bonn (grant no. O-137.0028, MW). We are grateful for the technical support of Carlo Pellizzari from CenterVue SpA (Padua, Italy), which provided research material (S-MAIA) necessary to conduct this study. CenterVue had no role in the design or conduct of the experiments.

Disclosure: **S.G. Ponderfer**, Heidelberg Engineering (F), Optos (F), Carl Zeiss Meditec (F), CenterVue (F); **M.W.M. Wintergerst**, Heidelberg Engineering (F), Optos (F), Carl Zeiss Meditec (F), CenterVue (F), Heine Optotechnik (C, F), DigiSight Technologies (F), D-Eye (F); **S. Gorgi Zadeh**, None; **T. Schultz**, None; **M. Heinemann**, Heidelberg Engineering (F), Optos (F), Carl Zeiss Meditec (F), CenterVue (F); **F.G. Holz**, Heidelberg Engineering (F, C, R), Optos (F), Carl Zeiss Meditec (F, C), CenterVue (F), Allergan (F, R), Alcon/Novartis (F, R), Genentech/Roche (F, R), Bayer (F, R), Acucela (F, R), Boehringer Ingelheim (F, R); **R.P. Finger**, Heidelberg Engineering (F), Optos (F), Carl Zeiss Meditec (F), CenterVue (F), Bayer (C), Novartis (F, C), Santen (C), Opthea (C), Novilion (C), Retina Implant (C), Oxford Innovation (C)

References

1. Wong WL, Su X, Li X, et al. Global prevalence of age-related macular degeneration and disease burden projection for 2020 and 2040: a systematic review and meta-analysis. *Lancet Glob Health*. 2014;2:e106–e116.
2. Vingerling JR, Dielemans I, Hofman A, et al. The prevalence of age-related maculopathy in the Rotterdam study. *Ophthalmology*. 1995;102:205–210.
3. Cocce KJ, Stinnett SS, Luhmann UFO, et al. Visual function metrics in early and intermediate dry age-related macular degeneration for use as clinical trial endpoints. *Am J Ophthalmol*. 2018;189:127–138.
4. Scilley K, Jackson GR, Cideciyan AV, Maguire MG, Jacobson SG, Owsley C. Early age-related maculopathy and self-reported visual difficulty in daily life. *Ophthalmology*. 2002;109:1235–1242.
5. Owsley C, McGwin G JR, Scilley K, Kallies K. Development of a questionnaire to assess vision problems under low luminance in age-related maculopathy. *Invest Ophthalmol Vis Sci*. 2006;47:528–535.
6. Dimitrov PN, Robman LD, Varsamidis M, et al. Visual function tests as potential biomarkers in age-related macular degeneration. *Invest Ophthalmol Vis Sci*. 2011;52:9457–9469.
7. Lim LS, Mitchell P, Seddon JM, Holz FG, Wong TY. Age-related macular degeneration. *Lancet*. 2012;379:1728–1738.
8. Spaide RF, Curcio CA. Drusen characterization with multimodal imaging. *Retina*. 2010;30:1441–1454.
9. Johnson PT, Lewis GP, Talaga KC, et al. Drusen-associated degeneration in the retina. *Invest Ophthalmol Vis Sci*. 2003;44:4481–4488.
10. Hageman GS, Luthert PJ, Victor Chong NH, Johnson LV, Anderson DH, Mullins RF. An integrated hypothesis

- that considers drusen as biomarkers of immune-mediated processes at the RPE-Bruch's membrane interface in aging and age-related macular degeneration. *Prog Retin Eye Res*. 2001;20:705–732.
11. Ferris FL, Wilkinson CP, Bird A, et al. Clinical classification of age-related macular degeneration. *Ophthalmology*. 2013;120:844–851.
 12. Klein R, Davis MD, Magli YL, Segal P, Klein BE, Hubbard L. The Wisconsin age-related maculopathy grading system. *Ophthalmology*. 1991;98:1128–1134.
 13. Ferris FL, Davis MD, Clemons TE, et al. A simplified severity scale for age-related macular degeneration: AREDS Report No. 18. *Arch Ophthalmol*. 2005;123:1570–1574.
 14. Gorgi Zadeh S, Wintergerst MWM, Wiens V, et al. CNNs enable accurate and fast segmentation of drusen in optical coherence tomography: deep learning in medical image analysis and multimodal learning for clinical decision support. *Lect Notes Comput Sci*. 2017:65–73.
 15. Gregori G, Wang F, Rosenfeld PJ, et al. Spectral domain optical coherence tomography imaging of drusen in nonexudative age-related macular degeneration. *Ophthalmology*. 2011;118:1373–1379.
 16. Nittala MG, Ruiz-Garcia H, Sadda SR. Accuracy and reproducibility of automated drusen segmentation in eyes with non-neovascular age-related macular degeneration. *Invest Ophthalmol Vis Sci*. 2012;53:8319–8324.
 17. Ferris FL, Kassoff A, Bresnick GH, Bailey I. New visual acuity charts for clinical research. *Am J Ophthalmol*. 1982;94:91–96.
 18. Sunness JS, Rubin GS, Broman A, Applegate CA, Bressler NM, Hawkins BS. Low luminance visual dysfunction as a predictor of subsequent visual acuity loss from geographic atrophy in age-related macular degeneration. *Ophthalmology*. 2008;115:1480–1488, 1488.e1–2.
 19. Shah N, Dakin SC, Dobinson S, Tufail A, Egan CA, Anderson RS. Visual acuity loss in patients with age-related macular degeneration measured using a novel high-pass letter chart. *Br J Ophthalmol*. 2016;100:1346–1352.
 20. Pelli DG, Robson JG, Wilkins AJ. The design of a new letter chart for measuring contrast sensitivity. *Clin Vis Sci*. 1988;2:187–199.
 21. Mantyjarvi M, Laitinen T. Normal values for the Pelli-Robson contrast sensitivity test. *J Cataract Refract Surg*. 2001;27:261–266.
 22. Maynard ML, Zele AJ, Feigl B. Mesopic Pelli-Robson contrast sensitivity and MP-1 microperimetry in healthy ageing and age-related macular degeneration. *Acta Ophthalmol*. 2016;94:e772–e778.
 23. Trauzettel-Klosinski S, Dietz K. Standardized assessment of reading performance: the New International Reading Speed Texts IReST. *Invest Ophthalmol Vis Sci*. 2012;53:5452–5461.
 24. Pfau M, Lindner M, Fleckenstein M, et al. Test-retest reliability of scotopic and mesopic fundus-controlled perimetry using a modified MAIA (macular integrity assessment) in normal Eyes. *Ophthalmologica*. 2017;237:42–54.
 25. Welker SG, Pfau M, Heinemann M, Schmitz-Valckenberg S, Holz FG, Finger RP. Retest reliability of mesopic and dark-adapted microperimetry in patients with intermediate age-related macular degeneration and age-matched controls. *Invest Ophthalmol Vis Sci*. 2018;59:AMD152–AMD159.
 26. Cormen TH, Leiserson CE, Rivest RK, Stein C. *Introduction to Algorithms*, 3rd ed. Cambridge, MA: MIT Press; 2009;658–663.
 27. IBM Corp. *IBM SPSS Statistics for Windows, Version 25.0*. Armonk, NY: IBM; 2017.
 28. Wu Z, Ayton LN, Makeyeva G, Guymer RH, Luu CD. Impact of reticular pseudodrusen on microperimetry and multifocal electroretinography in intermediate age-related macular degeneration. *Invest Ophthalmol Vis Sci*. 2015;56:2100–2106.
 29. Midea E, Vujosevic S, Convento E, Manfre' A, Cavarzeran F, Pilotto E. Microperimetry and fundus autofluorescence in patients with early age-related macular degeneration. *Br J Ophthalmol*. 2007;91:1499–1503.
 30. Hartmann KI, Bartsch D-UG, Cheng L, et al. Scanning laser ophthalmoscope imaging stabilized microperimetry in dry age-related macular degeneration. *Retina*. 2011;31:1323–1331.
 31. Acton JH, Smith RT, Hood DC, Greenstein VC. Relationship between retinal layer thickness and the visual field in early age-related macular degeneration. *Invest Ophthalmol Vis Sci*. 2012;53:7618–7624.
 32. Chandramohan A, Stinnett SS, Petrowski JT, et al. Visual function measures in early and intermediate age-related macular degeneration. *Retina*. 2016;36:1021–1031.
 33. Wu Z, Ayton LN, Guymer RH, Luu CD. Low-luminance visual acuity and microperimetry in age-related macular degeneration. *Ophthalmology*. 2014;121:1612–1619.
 34. Owsley C, Huisinigh C, Clark ME, Jackson GR, McGwin G, Jr. Comparison of visual function in older eyes in the earliest stages of age-related macular degeneration to those in normal macular health. *Curr Eye Res*. 2016;41:266–272.
 35. Klein R, Wang Q, Klein BE, Moss SE, Meuer SM. The relationship of age-related maculopathy, cataract, and glaucoma to visual acuity. *Invest Ophthalmol Vis Sci*. 1995;36:182–191.
 36. Chan H, Cougnard-Gregoire A, Delyfer M-N, et al. Multimodal imaging of reticular pseudodrusen in a population-based setting: the Alienor study. *Invest Ophthalmol Vis Sci*. 2016;57:3058–3065.
 37. Puell MC, Barrio AR, Palomo-Alvarez C, Gomez-Sanz FJ, Clement-Corral A, Perez-Carrasco MJ. Impaired mesopic visual acuity in eyes with early age-related macular degeneration. *Invest Ophthalmol Vis Sci*. 2012;53:7310–7314.
 38. Feigl B, Brown B, Lovie-Kitchin J, Swann P. Monitoring retinal function in early age-related maculopathy: visual performance after 1 year. *Eye (Lond)*. 2005;19:1169–1177.
 39. Nathoo NA, Or C, Young M, et al. Optical coherence tomography-based measurement of drusen load predicts development of advanced age-related macular degeneration. *Am J Ophthalmol*. 2014;158:757–761.e1.
 40. Complications of Age-related Macular Degeneration Prevention Trial (CAPT) Research Group. Risk factors for choroidal neovascularization and geographic atrophy in the complications of age-related macular degeneration prevention trial. *Ophthalmology*. 2008;115:1474–1479, 1479.e1–6.
 41. Seddon JM, Reynolds R, Yu Y, Daly MJ, Rosner B. Risk models for progression to advanced age-related macular degeneration using demographic, environmental, genetic, and ocular factors. *Ophthalmology*. 2011;118:2203–2211.
 42. Lei J, Balasubramanian S, Abdelfattah NS, Nittala MG, Sadda SR. Proposal of a simple optical coherence tomography-based scoring system for progression of age-related macular degeneration. *Graefes Arch Clin Exp Ophthalmol*. 2017;255:1551–1558.
 43. Yehoshua Z, Wang F, Rosenfeld PJ, Penha FM, Feuer WJ, Gregori G. Natural history of drusen morphology in age-related macular degeneration using spectral domain optical coherence tomography. *Ophthalmology*. 2011;118:2434–2441.
 44. Saßmannshausen M, Steinberg JS, Fimmers R, et al. Structure-function analysis in patients with intermediate age-related macular degeneration. *Invest Ophthalmol Vis Sci*. 2018;59:1599–1608.
 45. Pfau M, Müller PL, von der, L, et al. Mesopic and dark-adapted two-color fundus-controlled perimetry in

- geographic atrophy secondary to age-related macular degeneration. *Retina*. 2020;40:169–180.
46. Chen Q, Leng T, Zheng L, et al. Automated drusen segmentation and quantification in SD-OCT images. *Med Image Anal*. 2013;17:1058–1072.
47. Finger RP, Schmitz-Valckenberg S, Schmid M, et al. MACUS-TAR: development and clinical validation of functional, structural, and patient-reported endpoints in intermediate age-related macular degeneration. *Ophthalmologica*. 2019;241:61–72.